

Comment

# A Brief Commentary on the Interpretation of Chinese Speleothem $\delta^{18}\text{O}$ Records as Summer Monsoon Intensity Tracers

Daniel Gebregiorgis <sup>1,\*</sup>, Steven C. Clemens <sup>2</sup>, Ed C. Hathorne <sup>3</sup>, Liviu Giosan <sup>4</sup>,  
Kaustubh Thirumalai <sup>5</sup> and Martin Frank <sup>3</sup>

<sup>1</sup> Department of Geosciences, Georgia State University, Atlanta, GA 30302, USA

<sup>2</sup> Department of Geological Sciences, Brown University, Providence, RI 02912, USA;  
Steven\_Clemens@brown.edu

<sup>3</sup> GEOMAR Helmholtz Centre for Ocean Research Kiel, 24148 Kiel, Germany; ehathorne@geomar.de (E.C.H.);  
mfrank@geomar.de (M.F.)

<sup>4</sup> Department of Geology and Geophysics, Woods Hole Oceanographic Institution, Woods Hole, MA 02543,  
USA; lgiosan@whoi.edu

<sup>5</sup> Department of Geosciences, University of Arizona, Tucson, AZ 85721, USA; kaustubh@email.arizona.edu

\* Correspondence: dgebregiorgis@gsu.edu

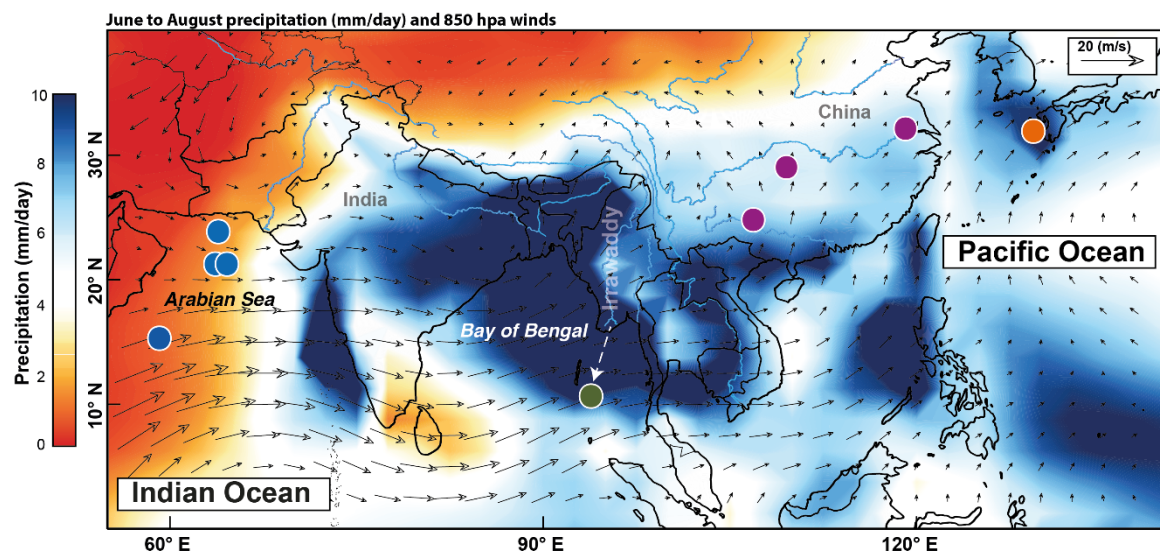
Received: 31 October 2019; Accepted: 16 January 2020; Published: 18 March 2020



Zhang et al. [1] argue that changes in northern hemisphere summer insolation (NHSI) caused by the precession of Earth's orbit have controlled the timing and pace of the late Pleistocene East Asian summer monsoon (EASM) and Indian summer monsoon (ISM). Since the early 2000s, several high-resolution cave  $\delta^{18}\text{O}$  records from China dated with unprecedented precision have been published [2–5] and are widely interpreted as proxies for East Asian summer monsoon (EASM) intensity [5]. Modern observations, however, do not demonstrate a clear relationship between the amount of precipitation and the  $\delta^{18}\text{O}$  signature in cave drip water [6–8]. There is no modern analogue for the spatially homogenous ‘rainfall’ patterns inferred from the cave  $\delta^{18}\text{O}$  records [6], and mass-balance calculations demonstrate that the range of cave  $\delta^{18}\text{O}$  variations requires unfeasibly high changes in rainfall [9]. The cave  $\delta^{18}\text{O}$  records are also inconsistent with other published proxy records of EASM rainfall based on Chinese Loess magnetic records [9] and beryllium isotopes [10]. The interpretation that negative excursions in the cave  $\delta^{18}\text{O}$  records reflect changes in the amount of monsoon rainfall alone is only partially supported [11,12] and remains widely contested [13]. The Zhang et al. study also does not address evidence from recently published marine and terrestrial proxy records of monsoon precipitation from the EASM and ISM domains [14,15], which are at odds with the major conclusions drawn therein [1].

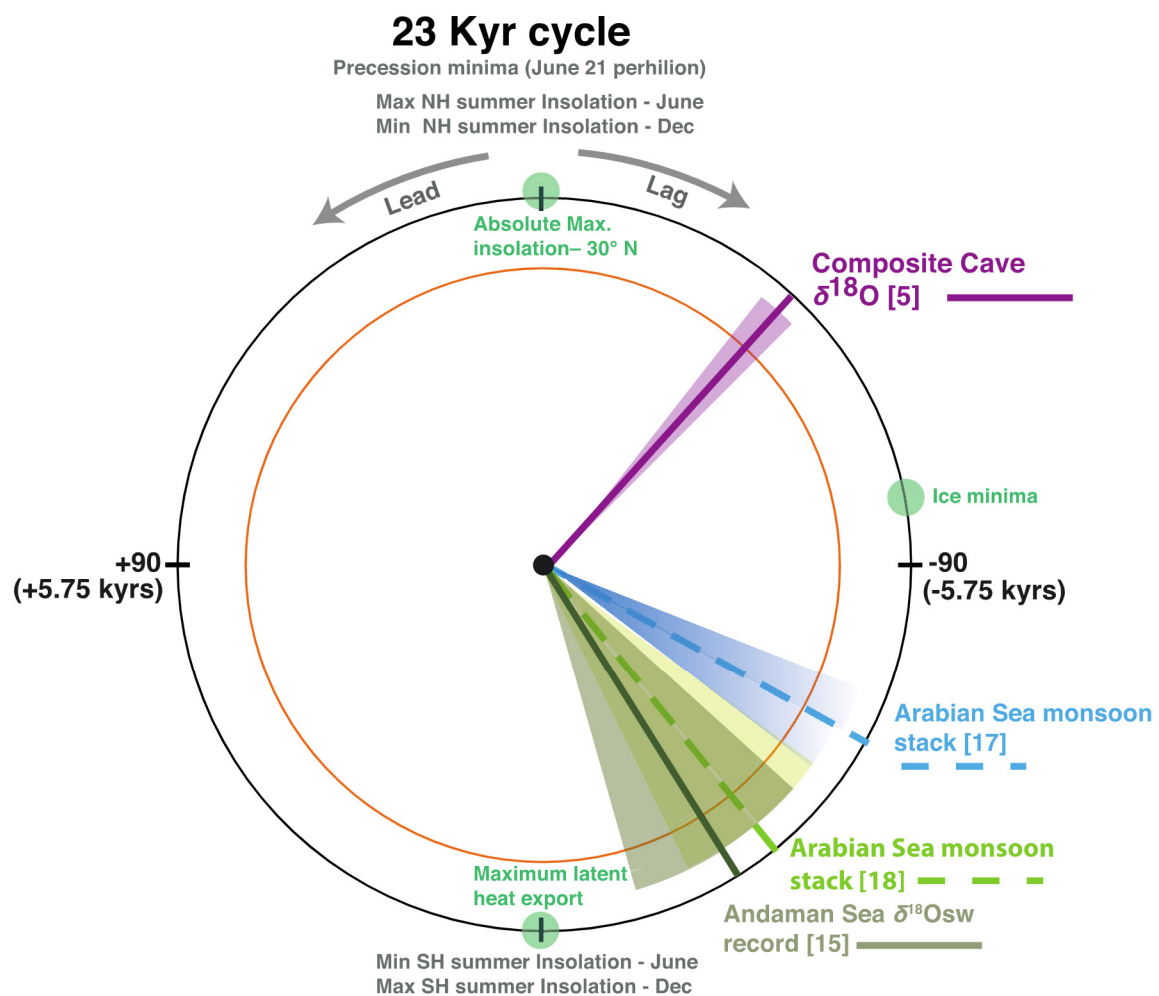
Early reconstructions of Asian summer monsoon intensity were based on proxies of wind strength over the Arabian Sea [16–18]. These results were interpreted to infer changes in the intensity of monsoon precipitation over land given that strong summer monsoon winds promote upwelling-driven productivity in the Arabian Sea [19], and transport large amounts of moisture to the Asian continent [20]. More recently, seawater  $\delta^{18}\text{O}$  ( $\delta^{18}\text{O}_{\text{sw}}$ ) records from important monsoon sink regions such as the East China Sea [14] and the Andaman Sea [15] have been published (Figure 1). These reconstructions reflect changes in regional rainfall integrated over large river basins and the open ocean. Gebregiorgis et al., [15] showed that Pleistocene Andaman Sea  $\delta^{18}\text{O}_{\text{sw}}$  variability has the same late precession-band phase as the Arabian Sea wind records [16–18], confirming the link between the summer monsoon winds in the Arabian Sea and rainfall in the larger Bay of Bengal region. Unlike speleothem  $\delta^{18}\text{O}$ , the Arabian Sea and Andaman ISM records lag NHSI maxima by ~8 kyrs, which delineates ISM sensitivity to global ice volume as well as Southern Hemisphere moisture and energy export [16–18]. The phase wheel

diagram in Figure 2 illustrates the precession phasing of marine and speleothem based EASM and ISM reconstructions.



**Figure 1.** June–August mean precipitation (mm/day) and 850-hPa winds in the Asian monsoon domain for the period 1979–2015 (GPCC precipitation data provided by the NOAA/OAR/ESRL PSD and can be accessed at <https://www.esrl.noaa.gov/psd/>). Orange and green filled circle shows the location of marine core sites in the East China Sea [14] and the Andaman Sea [15]. Purple filled circles show the locations of the three main Chinese caves (Dongge cave–Southern China; Sanbao cave–Central China; and Hulu cave–Eastern China) [4]. Also shown are some of the Arabian Sea marine core sites (all in blue) from [17,18].

The conclusion of Zhang et al. [1] that EASM and ISM variability on orbital timescales has been driven directly by changes in Northern Hemisphere summer insolation without significant temporal lags is entirely inconsistent with the EASM  $\delta^{18}\text{O}_{\text{sw}}$  reconstruction from the East China Sea [14]. This record shows no concentration of variance in the precession band once the temperature and ice-volume influence on foraminiferal-calcite  $\delta^{18}\text{O}$  are removed and, hence, cannot be plotted on Figure 2. It is also inconsistent with the Andaman Sea  $\delta^{18}\text{O}_{\text{sw}}$  record, which closely follows the timing of the Arabian Sea precession band phase [15]. Zhang et al. do not present a discussion of these strongly divergent results and interpretations, which were both derived from the same isotopic system and archive ( $\delta^{18}\text{O}$  of  $\text{CaCO}_3$ ) in the same monsoon regions. Given that large-scale atmospheric circulation controls the transport of moisture between sources and sinks, the resultant speleothem  $\delta^{18}\text{O}$  signal likely reflects changes in moisture sources and pathways [9,21] or land-surface temperature or other processes [22], whereas the seawater  $\delta^{18}\text{O}$  signature in marginal basins reflects the amount and timing of regional monsoon rainfall.



**Figure 2.** Precession phasing of marine and speleothem-based reconstructions of the ISM and EASM. In the phase wheel representation, the 12 o'clock position denotes minimum precession (maximum NH insolation during the boreal summer). Phase lags increase in a clockwise direction; the 3 o'clock position represents a 90° or 5.75 kyrs phase lag. Maximum latent heat export from the southern subtropical Indian Ocean is at −180° [17,18]. Green filled circles show the timing of potential summer monsoon forcing mechanisms and include the absolute maximum insolation over Asia [23], minimum ice volume [23], and maximum export of latent heat from the southern subtropical Indian Ocean [17,18].

**Author Contributions:** All authors contributed equally to this work. All authors have read and agreed to the published version of the manuscript.

**Funding:** This work received no external funding.

**Conflicts of Interest:** The authors declare that there are no conflicts of interest.

## References

1. Zhang, H.; Ait Brahimi, Y.; Li, H.; Zhao, J.; Kathayat, G.; Tian, Y.; Edwards, R.L. The Asian Summer Monsoon: Teleconnections and Forcing Mechanisms—A Review from Chinese Speleothem  $\delta^{18}\text{O}$  Records. *Quaternary* **2019**, *2*, 26. [CrossRef]
2. Wang, Y.J.; Cheng, H.; Edwards, R.L.; An, Z.S.; Wu, J.Y.; Shen, C.C.; Dorale, J.A. A high-resolution absolute-dated Late Pleistocene monsoon record from Hulu Cave, China. *Science* **2001**, *294*, 2345–2348. [CrossRef] [PubMed]
3. Wang, Y.; Cheng, H.; Edwards, R.L.; Kong, X.; Shao, X.; Chen, S.; An, Z. Millennial- and orbital- scale changes in the East Asian Monsoon over the past 224,000 years. *Nature* **2008**, *451*, 1090–1093. [CrossRef] [PubMed]

4. Cheng, H.; Edwards, R.L.; Broecker, W.S.; Denton, G.H.; Kong, X.; Wang, Y.; Wang, X. Ice age terminations. *Science* **2009**, *326*, 248–252. [[CrossRef](#)] [[PubMed](#)]
5. Cheng, H.; Edwards, R.L.; Sinha, A.; Spötl, C.; Yi, L.; Chen, S.; Kong, X. The Asian monsoon over the past 640,000 years and ice age terminations. *Nature* **2016**, *534*, 640–646. [[CrossRef](#)] [[PubMed](#)]
6. Dayem, K.E.; Molnar, P.; Battisti, D.S.; Roe, G.H. Lessons learned from oxygen isotopes in modern precipitation applied to interpretation of speleothem records of paleoclimate from eastern Asia. *Earth Planet. Sci. Lett.* **2010**, *295*, 219–230. [[CrossRef](#)]
7. Tan, M. Circulation effect: Response of precipitation  $\delta^{18}\text{O}$  to the ENSO cycle in monsoon regions of China. *Clim. Dyn.* **2014**, *42*, 1067–1077. [[CrossRef](#)]
8. Sun, Z.; Yang, Y.; Zhao, J.; Tian, N.; Feng, X. Potential ENSO effects on the oxygen isotope composition of modern speleothems: Observations from Jiguan Cave, central China. *J. Hydrol.* **2018**, *566*, 164–174. [[CrossRef](#)]
9. Maher, B.A.; Thompson, R. Oxygen isotopes from Chinese caves: Records not of monsoon rainfall but of circulation regime. *J. Quat. Sci.* **2012**, *27*, 615–624. [[CrossRef](#)]
10. Beck, J.W.; Zhou, W.; Li, C.; Wu, Z.; White, L.; Xian, F.; Kong, X.; An, Z. A 550,000-year record of East Asian monsoon rainfall from 10Be in loess. *Science* **2018**, *360*, 877–881. [[CrossRef](#)]
11. Liu, Z.; Wen, X.; Brady, E.C.; Otto-Bliesner, B.; Yu, G.; Lu, H.; Edwards, R.L. Chinese cave records and the East Asia summer monsoon. *Quat. Sci. Rev.* **2014**, *83*, 115–128. [[CrossRef](#)]
12. Pausata, F.S.; Battisti, D.S.; Nisancioglu, K.H.; Bitz, C.M. Chinese stalagmite  $\delta^{18}\text{O}$  controlled by changes in the Indian monsoon during a simulated Heinrich event. *Nat. Geosci.* **2011**, *4*, 474. [[CrossRef](#)]
13. Clemens, S.C.; Prell, W.L.; Sun, Y. Orbital-scale timing and mechanisms driving Late Pleistocene Indo-Asian summer monsoons: Reinterpreting cave speleothem  $\delta^{18}\text{O}$ . *Paleoceanography* **2010**, *25*. [[CrossRef](#)]
14. Clemens, S.C.; Holbourn, A.; Kubota, Y.; Lee, K.E.; Liu, Z.; Chen, G.; Fox-Kemper, B. Precession-band variance missing from East Asia monsoon runoff. *Nat. Commun.* **2018**, *9*, 3364. [[CrossRef](#)] [[PubMed](#)]
15. Gebregiorgis, D.; Hathorne, E.C.; Giosan, L.; Clemens, S.; Nürnberg, D.; Frank, M. Southern Hemisphere forcing of South Asian monsoon precipitation over the past~ 1 million years. *Nat. Commun.* **2018**, *9*, 4702. [[CrossRef](#)] [[PubMed](#)]
16. Clemens, S.C.; Prell, W.; Murray, D.; Shimmield, G.; Weedon, G. Forcing mechanisms of the Indian Ocean monsoon. *Nature* **1991**, *353*, 720–725. [[CrossRef](#)]
17. Clemens, S.C.; Prell, W.L. A 350,000 year summer-monsoon multi- proxy stack from the Owen Ridge, Northern Arabian Sea. *Mar. Geol.* **2003**, *201*, 35–51. [[CrossRef](#)]
18. Caley, T.; Malaizé, B.; Zaragosi, S.; Rossignol, L.; Bourget, J.; Eynaud, F.; Ellouz-Zimmermann, N. New Arabian Sea records help decipher orbital timing of Indo-Asian monsoon. *Earth Planet. Sci. Lett.* **2011**, *308*, 433–444. [[CrossRef](#)]
19. Murtugudde, R.; Seager, R.; Thoppil, P. Arabian Sea response to monsoon variations. *Paleoceanography* **2007**, *22*. [[CrossRef](#)]
20. Wang, P.X.; Wang, B.; Cheng, H.; Fasullo, J.; Guo, Z.; Kiefer, T.; Liu, Z. The global monsoon across time scales: Mechanisms and outstanding issues. *Earth Sci. Rev.* **2017**, *174*, 84–121. [[CrossRef](#)]
21. Caley, T.; Roche, D.M.; Renssen, H. Orbital Asian summer monsoon dynamics revealed using an isotope-enabled global climate model. *Nat. Commun.* **2014**, *5*, 5371. [[CrossRef](#)] [[PubMed](#)]
22. Battisti, D.S.; Ding, Q.; Roe, G.H. Coherent pan-Asian climatic and isotopic response to orbital forcing of tropical insolation. *J. Geophys. Res. Atmos.* **2014**, *119*, 11–997. [[CrossRef](#)]
23. Prell, W.L.; Kutzbach, J.E. Sensitivity of the Indian monsoon to forcing 104 parameters and implications for its evolution. *Nature* **1992**, *360*, 647–652. [[CrossRef](#)]

